Biosensors and Bioelectronics 142 (2019) 111496

Contents lists available at ScienceDirect

Biosensors and Bioelectronics

journal homepage: www.elsevier.com/locate/bios

Lamb wave-based molecular diagnosis using DNA hydrogel formation by rolling circle amplification (RCA) process

Jeonghun Nam[a,b,*,1], Woong Sik Jang[a,b,1], Jisu Kim[c], Hyukjin Lee[c], Chae Seung Lim[a,**]

[a] Department of Laboratory Medicine, College of Medicine, Korea University, Seoul, South Korea
[b] Department of Emergency Medicine, College of Medicine, Korea University, Seoul, South Korea
[c] College of Pharmacy, Graduate School of Pharmaceutical Sciences, Ewha Womans University, Seoul, South Korea

ARTICLE INFO

Keywords:
Lamb wave
Molecular diagnosis
Gene amplification
DNA hydrogel
Acoustic streaming

ABSTRACT

Recent developments in microfluidics enable the lab-on-a-chip-based molecular diagnosis. Rapid and accurate diagnosis of infectious diseases is critical for preventing the transmission of the disease. Here, we characterize a Lamb wave-based device using various parameters including the contact angle and viscosity of the sample droplet, the applied voltage, and the temperature increase. Additionally, we demonstrate the functionality of the Lamb wave-based device in clinical application. Optimal temperature for rolling circle amplification (RCA) process is 30 °C, and it was achieved by Lamb wave generation at 17 V. Gene amplification due to RCA process could be detected by viscosity increase due to DNA hydrogel formation in a sample droplet, which induced the acoustic streaming velocity of suspended particles to be decreased. In our Lamb wave-based device, isothermal amplification of target nucleic acids could be successfully detected within 30 min using 10 μL of sessile droplet, and was validated by comparing that of commercial real-time fluorescence analysis. Our device enables simple and low-cost molecular diagnosis, which can be applied to resource-limited clinical settings.

1. Introduction

Rapid and accurate diagnosis of infectious diseases, such as malaria, dengue, MERS, Ebola, and Zika, is critical to prevention of further transmission and appropriate treatments to the patients, which can reduce mortality (Allegranzi et al., 2011). Previously, tissue culture method has been considered as the standard diagnostic technique, which was limited due to time-consuming and labor-intensive processing. According to recent development of molecular diagnostic techniques, nucleic acid amplification tests (NAATs) have higher detection sensitivity and specificity, especially in a low prevalence population of infectious pathogens. Among amplification methods including polymerase chain reaction (PCR), strand displacement assay (SDA), and transcription mediated assay (TMA) (Guerrant et al., 2011), PCR-based diagnosis has been most widely used (Loman et al., 2012). However, conventional PCR requires an expensive and large benchtop instrument, which is not applicable to point-of-care (POC) testing or resource-limited environments.

Microfluidic techniques have been drastically improved and have gained much attention for molecular diagnosis due to their advantages, such as small sample and reagent volume and fast reaction time. Recently, novel microfluidic systems for pathogen detection based on DNA hydrogel formation during rolling circle amplification (RCA) have been proposed by blocked microfluidic in the microfluidic array chip (Lee et al., 2015), and blocked flow path between packed beads in the microchannel (Na et al., 2018). However, these methods require a time-consuming preparation process using expensive instruments for the primer immobilization in the microchannel or on the beads, and bead filling process by skilled personnel. Therefore, it is essential to develop a microfluidic device for pathogen detection without complex and time-consuming device preparation process.

Among various microfluidic techniques, acoustic wave-based microfluidic devices have been widely used due to label-free, non-invasive manipulation with low power consumption. Guttenberg et al. proposed a microfluidic device for PCR using a thin film resistance heater combined with the surface acoustic wave (SAW) technique for driving the sample droplet to the heater and mixing the sample during PCR (Guttenberg et al., 2005). Rebound et al. proposed a SAW-based cell lysis and PCR amplification device (Reboud et al., 2012). Heating induced by SAW actuation could generate cyclic temperature changes

* Corresponding author. Department of Laboratory Medicine, College of Medicine, Korea University, 226 Gamasan-ro, Guro-gu, Seoul, 08307, South Korea.
** Corresponding author. Department of Laboratory Medicine, College of Medicine, Korea University, 226 Gamasan-ro, Guro-gu, Seoul, 08307, South Korea.
E-mail addresses: namjh@korea.ac.kr (J. Nam), malarim@korea.ac.kr (C.S. Lim).
[1] These authors contributed equally to this work.

https://doi.org/10.1016/j.bios.2019.111496
Received 20 February 2019; Received in revised form 10 May 2019; Accepted 7 July 2019
Available online 10 July 2019
0956-5663/

which satisfied the stepwise PCR protocols. Furthermore, a SAW-based multiplexed loop-mediated isothermal amplification (LAMP) was demonstrated to detect sexually transmitted diseases (Xu et al., 2015).

By using SAW technique, heat generation and acoustic streaming-induced mixing can be simultaneously utilized, which can enhance the amplification process. However, from these SAW-based PCR devices, fluorescence intensity should be measured to evaluate the PCR product. In addition, to generate SAW actuation, metal electrodes are required to be patterned on a piezoelectric material by using costly cleanroom facilities for metal deposition, lithographic and etching processes.

Recently, to address the limitations of SAW actuation, a Lamb wave-based device was proposed, and it demonstrated only fundamental studies on acoustic streaming, mixing, particle patterning, and sorting in a sessile droplet (Destgeer et al., 2016; Rezk et al., 2014; Yeo and Rezk, 2017). Meanwhile, clinical application of the Lamb wave-based device on blood analysis, especially blood coagulation assay, was recently reported by our group for the first time (Nam et al., 2018). In the Lamb wave-based device, blood coagulation test was conducted based on the typical index of blood coagulation, Prothrombin time (PT), in approximately 30 s, during which consideration of evaporation of the droplet was not needed. For efficient manipulation of the droplet in the Lamb wave-based device, improvement of the device by parametric studies on device configurations and experimental conditions are still required. In addition, to the best of the authors' knowledge, the Lamb wave-based device has not been applied to clinical molecular diagnosis.

In this study, we propose a Lamb wave-based device for clinical molecular diagnostic application based on DNA hydrogel formation by rolling circle amplification (RCA). Various experimental parameters, such as viscosity and contact angle of the sample liquid, and the relation between applied voltage and temperature, are studied. In this short communication, as proof-of-concept, products from isothermal gene amplification process in RCA method are monitored to detect dengue virus by analyzing Lamb wave-induced acoustic streaming of suspended particles in the sample.

2. Experimental

2.1. Working principle

Fig. 1 depicts the device and the working principle of the Lamb wave-based DNA amplification. Fig. 1(a) shows a schematic of the Lamb wave device, containing the piezoelectric substrate (lithium niobate, $LiNbO_3$, 128°, Y-cut, X-propagation, NEL Crystal Co., Fukushima) with aluminum tape electrodes on the bottom surface and a PDMS open chamber. As a pair of electrodes, aluminum tape was cut into a rectangular shape of ~6 × 75 mm. The PDMS open chamber is filled with mineral oil to prevent the evaporation of the sample during DNA amplification process by covering the sample droplets. To prevent the droplet from moving during the experiment, the surface of the piezoelectric substrate is treated with a hydrophobic material (trichloro (1H,1H,2H, 2H-perfluorooctyl)silane, OTS, Sigma Aldrich) by using a microstamping method (Romanov et al., 2014; Zilio et al., 2014). Briefly, PDMS stamps containing patterns with a 3-mm diameter circular exclusion can be fabricated by soft lithography. After creating the stamp, the hydrophobic material is transferred onto the surface of the stamp and printed by contact. Fig. 1(b) shows an image of the Lamb wave-based DNA amplification device used in this study.

By applying a radio-frequency (RF) signal to the aluminum tape electrodes, Lamb wave is induced throughout the piezoelectric substrate. Resonant frequency of the Lamb wave device depends only on the thickness of the piezoelectric substrate following the equation:

$$f = \frac{c}{\lambda}$$

where f, c, and λ are the resonance frequency, the speed of sound along the $LiNbO_3$ substrate (~3900 m/s), and the wavelength, respectively.

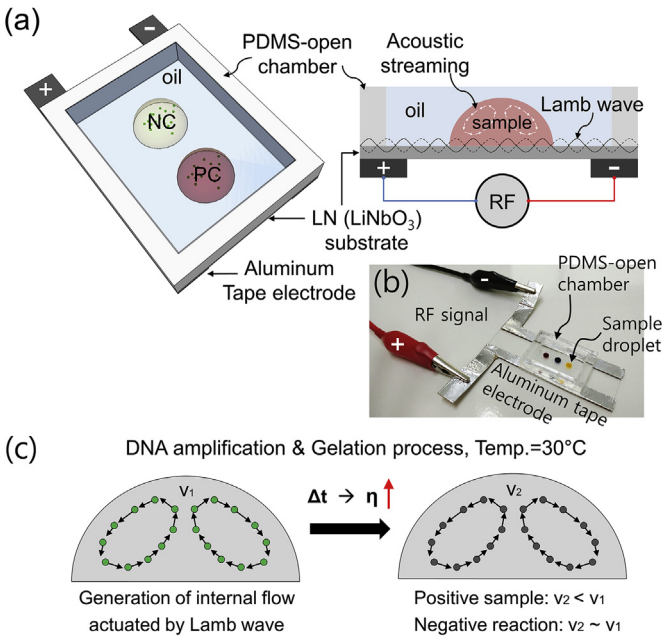

Fig. 1. (a) Schematic of Lamb-wave based DNA amplification device containing a piezoelectric substrate, aluminum tape electrodes, and a PDMS open chamber. By applying a radio frequency (RF) signal, Lamb wave is generated throughout the substrate, which can induce acoustic streaming in a sample droplet. (b) Image of the Lamb wave-based DNA amplification device used in this study. (c) By Lamb wave, internal flow is actuated in the droplet, which can be visualized by streaming of suspended particles with streaming velocity v_1. Due to the gelation during DNA amplification process (Δt), viscoelasticity of the sample droplet increases and streaming velocity of suspended particles becomes decreased to v_2 in a positive sample, while that of a negative sample remains similar to the initial streaming velocity.

The wavelength of the Lamb wave can be determined by the thickness of the $LiNbO_3$ substrate (T) from the relation $T = \lambda/2$ (Yeo and Rezk, 2017). Among the successive harmonic resonant frequencies $(2n + 1)\lambda/2$ (n = 0, 1, 2, …), the applied frequency to the silver paste electrodes was determined as 173.3 MHz.

During the gene amplification process, RCA products are generated by isothermal amplification process and self-assembled to form a DNA hydrogel. The DNA hydrogel continues to increment during the process, so that viscoelasticity of the sample droplet increases. To visualize the Lamb wave-induced acoustic streaming, fluorescent polystyrene particles are initially suspended in the sample droplet. As shown in Fig. 1(c), at the beginning of Lamb wave generation, the internal flow is generated with streaming velocity of suspended particles v_1. As the RCA reaction continues, the acoustic streaming velocity of suspended particles becomes decreasing into $v_{2,\ positive}$ due to the viscosity increase in a positive sample. A suspended particle experiences drag force during the acoustic streaming as shown below:

$$F_D = 6\pi\mu Ur$$

where μ, U, and r are the fluid dynamic viscosity, streaming velocity, and particle radius, respectively. Therefore, the acoustic streaming velocity is inversely proportional to the fluid viscosity ($U \propto 1/\mu$). However, the acoustic streaming velocity in a negative sample ($v_{2,\ negative}$) remains similar to the initial streaming velocity (v_1).

2.2. Sample preparation

To evaluate temperature and acoustic streaming velocity depending on the applied voltages, a 10 μL droplet of deionized (DI) water was used. To visualize the acoustic streaming in the droplet, 5 μm fluorescent particles were suspended at the final concentration of 1.6 × 10^5

particles/mL.

2.3. The RCA reaction

For detection of dengue virus, we adopted the previous padlock design to form a DNA hydrogel (Jung et al., 2016). Dengue virus binding sequence in the padlock was designed to target the 3′ untranslated region of all complete genome sequences of dengue virus serotype 1–4 in this study. All the oligonucleotide sequences used in this study are listed in Table S1. In the dengue template, the segments at the 5′ end (11 bases) and the 3′ end (9 bases) were complementary to the dengue pathogen sequence, resulting in hybridization of the Dengue pathogen with the template and forming a circular structure. For RCA reaction, 1 μL of 100 μM dengue single-stranded DNA templates with a hydroxyl group at a 3′ was mixed with 1 μL of 100 μM dengue pathogen DNA, 1 μL of 10 μM primer, 1 μL of T4 ligase (400 U/μL), 1 μL of pyrophosphatase (100 U/mL), 4 μL of Phi29 DNA polymerase (10 U/μL), 4 μL of 10× phi29 polymerase buffer, 1 μL of 100 mM DTT, 4 μL of 25 mM dNTP, 1 μL of 50 mM ATP, 1 μL of BSA (10 mg/mL), and 22 μL of distilled water. The dengue RCA mixture was directly applied for Lamb-wave based DNA amplification device. For real-time fluorescence analysis, 1 μL of SYBR Green II was added to the mixture and then RCA product was visualized at 30 °C for 60 min by using a thermal cycler (Bio-Rad CFX96, Germany).

2.4. Experimental setup

To generate Lamb wave through the piezoelectric substrate, an RF signal was applied to silver paste electrodes by a signal generator (8657B, HP) with an amplifier (ZHL-1-2W, Mini-circuits) connected to a DC power supply (IPS–18B10, VuPOWER). During the experiment, internal streaming of suspended microparticles was observed by an inverted microscope (CKX41, Olympus) with a high-speed camera (V611, Phantom) for measuring streaming velocity, and a fluorescent camera (CS230B, Olympus) for monitoring gene amplification. The temperature in the sample droplet was recorded using a thermal imaging camera (FLIR one, FLIR Systems) after thermal saturation (~10 s).

3. Results and discussion

To examine the effect of contact angles on the acoustic streaming velocity of the suspended particles, the contact angle of the sample droplet was modulated as 15, 30, 45, 60, 75, 90°. Various contact angles of 10 μL droplet could be achieved by relatively hydrophilic circular area with different diameters (φ), as shown in Fig. 2(a). For desirable contact angles, the diameter of each droplet was calculated as follows (Yonemoto and Kunugi, 2014):

$$\frac{\rho_l g h V}{2} = \pi R^2 \sigma_{lg}(1 - \cos\theta) - \pi R h \sigma_{lg} \sin\theta$$

$$V = \pi h\left(\frac{h^2}{6} + \frac{R^2}{2}\right)$$

where ρ_l, g h, V, R, σ_{lg}, and θ are liquid density, gravitational acceleration, droplet height, droplet volume, droplet radius, liquid surface energy, and contact angle, respectively. According to the equation, the calculated diameters were 7.77, 6.01, 5.16, 4.60, 4.18, and 3.84 mm, respectively for contact angles 15, 30, 45, 60, 75, and 90°. The contact angles were confirmed by capturing the images from the side using a USB camera (800× Digital microscope, DMicroscope Inc.), as shown in Fig. 2(b). Measured contact angles were 14.9 ± 0.4°, 30.2 ± 0.3°, 44.4 ± 0.5°, 60.3 ± 0.4°, 75.2 ± 0.3°, and 89.7 ± 0.2°, respectively. The difference between the desired and the measured contact angles was smaller than ~0.5°.

Using the Lamb wave-based device shown in Fig. 2(a), the acoustic streaming velocity of the suspended 5 μm particles in DI water was measured depending on the contact angle at 16 V. The applied voltage of 16 V was chosen arbitrarily to induce the acoustic streaming velocity in the droplets. The acoustic streaming velocity can be examined by image analysis using the free video analysis and modelling tool Tracker 5.0 (Brown, 2012). Results are presented as average and standard deviation of velocity measurement from five separate droplets. As shown in Fig. 2(c), the acoustic streaming velocity increased from 3.8 μm/s to 121.5 μm/s, as the contact angle increased from 15° to 90°. In droplets with smaller contact angle, we assume that the acoustic streaming velocity decreases due to lower pressure gradient in the droplet induced by Lamb wave (Luong and Nguyen, 2010; Destgeer et al., 2017). In our experimental setup, highest acoustic streaming velocity could be achieved at the fixed applied voltage in the droplet with contact angle ~90°.

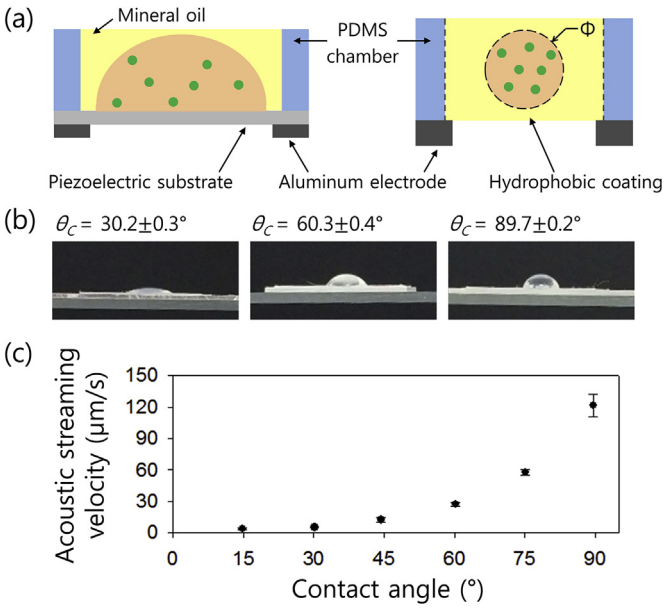

Fig. 2. (a) Schematic of the cross-sectional (left) and top (right) view of the Lamb wave-based device, respectively. (b) Photographs of the contact angle obtained from different droplets with different diameters but same volume (10 μL), which were side view images. (c) Acoustic streaming velocities of 5 μm fluorescent particles suspended in deionized (DI) water with varying contact angles at 16 V (n = 5).

Supplementary data related to this article can be found at https://doi.org/10.1016/j.bios.2019.111496.

To achieve RCA products by isothermal amplification process, the temperature of the sample droplet should be controlled at ~30 °C. Therefore, to determine the appropriate applied voltage for RCA reaction in the droplet in the present setup, temperature was measured with increasing voltages ranging from 14 to 24 V using the thermal imaging camera, as shown in Fig. 3(a). The diameter of the dispensed 10 μL sample droplet (D) to achieve the highest acoustic streaming velocity at the contact angle of 90° was 3.84 mm. Before the Lamb wave generation, the temperature of the sample was approximately 25 °C. The temperature was measured from the thermal image after 10 s for thermal saturation and averaged from five different droplets. At 14 V, the temperature was 25.4 °C, which is the same as room temperature. As the applied voltage increased to 17 V, the average temperature reached 30 °C, which is the optimal temperature for isothermal RCA process in this study. Once the applied voltage increased further to 24 V, the temperature reached 40 °C. For further experiments, the diameter of the droplet and the applied voltage were fixed as 3.84 mm and 17 V, respectively, to achieve a contact angle of 90° and a temperature of 30 °C. In addition, blue dots in Fig. 3(a) show the measured acoustic streaming velocities of suspended particles in DI water. The acoustic streaming velocity (v) increased from 101.4 μm/s at 14 V to 421.7 μm/s

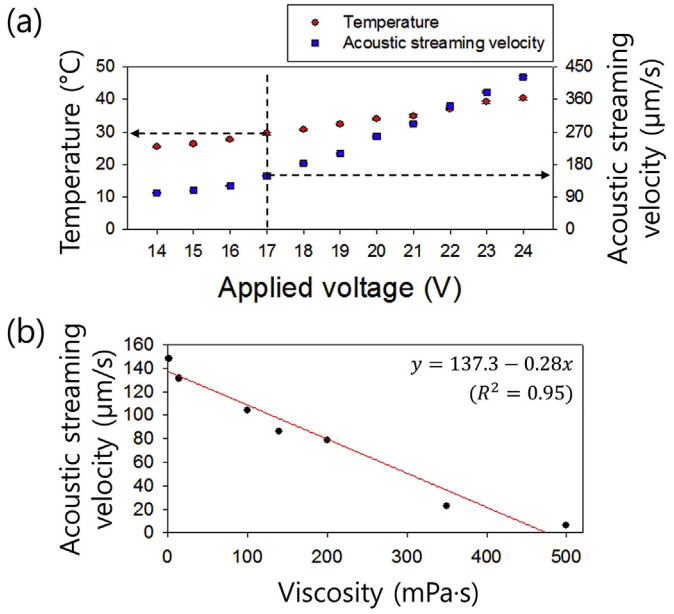

Fig. 3. (a) Temperatures measured in the droplet and acoustic streaming velocities of 5 μm fluorescent particles suspended in DI water at different applied voltages (n = 5). (b) Acoustic streaming velocities of 5 μm fluorescent particles suspended in glycerine solution with various viscosities at 17 V (n = 5).

at 24 V, which is theoretically proportional to the quadrature of the applied voltage (V^2).

To examine the effect of viscosity increase on the acoustic streaming velocity of the suspended particles, an aqueous solution of glycerine (G1345.1000, Duchefa Biochemie) was prepared in several viscosities, from 1.4 mPa s to 500 mPa s (1.4, 14, 100, 140, 200, 350, and 500 mPa s). Fig. 3(b) shows the acoustic streaming velocity of suspended particles decreasing from 148.4 μm/s to 5.85 μm/s, as the viscosity increases from 1.4 mPa s to 500 mPa s. Results are presented as the averaged velocities and the standard deviation from five separate droplets. In glycerine solution with the viscosity higher than 500 mPa s, no acoustic streaming of suspended particles was observed due to high viscosity of the suspending medium. Therefore, acoustic streaming velocities became almost 0. Acoustic streaming velocity of particles suspended in 1.4 mPa s glycerine solution was 148.4 μm/s at 17 V, which was almost same as that of particles suspended in DI water (viscosity ~ 0.9 mPa s at 25 °C). Lamb wave-induced acoustic streaming velocity is affected by the viscosity of the droplet according to the relation of $y = 137.3–0.28x$.

As proof-of-concept of the Lamb wave-based device for clinical application, dengue virus molecular amplification by RCA method was monitored. To monitor viscoelasticity changes due to DNA hydrogel formation during the RCA process, acoustic streaming velocity of fluorescent particles was measured at different times at 17 V. Fig. 4(a) shows the time-dependent acoustic streaming velocity results for negative sample (no dengue pathogen oligonucleotides) and dengue positive sample containing about 6×10^{13} copies of dengue pathogen oligonucleotides (100 pmol/μL). To validate the applicability of Lamb wave-based device to molecular analysis, pathogen DNA at an extreme concentration was used for proof-of-concept.

Time-dependent acoustic streaming velocities were measured every 5 min for 60 min, as shown in Fig. 4(a). Results are presented as the averaged velocities and the standard deviation from five separate droplets, and the acoustic streaming velocities were normalized by the maximum velocity of each sample. By virtue of the mineral oil filled in the PDMS open chamber, Lamb wave-based monitoring on RCA process could be continued for 60 min without droplet evaporation.

For the negative sample without target DNA in the sample droplet,

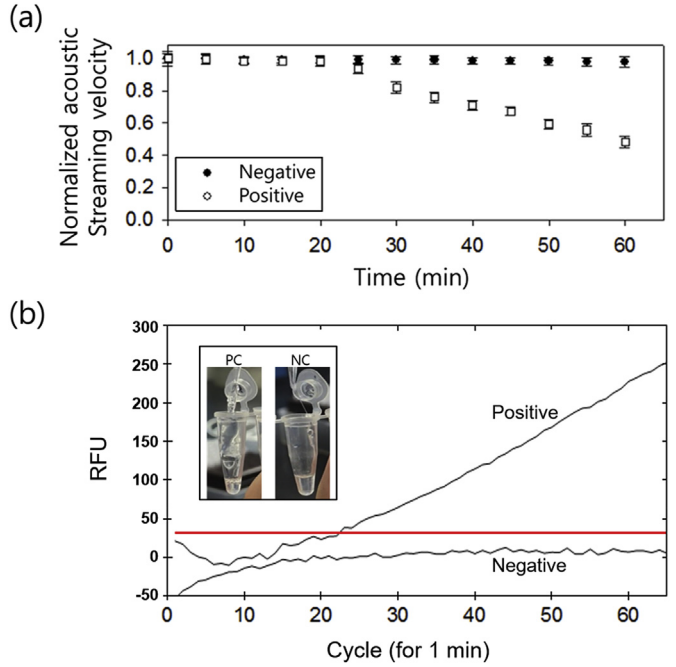

Fig. 4. (a) Normalized acoustic streaming velocities of 5 μm fluorescent particles suspended in dengue negative and dengue positive control, respectively at 17 V ($n = 5$). (b) Real-time fluorescence analysis on dengue negative and dengue positive control. Inset panel indicates DNA hydrogel formation by template DNA with dengue pathogen DNA (PC) and without dengue pathogen DNA (NC) after incubated at 30 °C for 8 h. PC: Positive, NC: Negative.

no RCA products were generated, and DNA hydrogel could not be formed. Therefore, the acoustic streaming velocity remained uniform and the normalized velocities maintained at almost 1 for 60 min, since there was no gelation-induced viscoelasticity increase.

On the contrary, the acoustic streaming velocities of particles suspended in positive controls containing target DNA showed distinct changes during the process. Normalized acoustic streaming velocity remained almost constant for 20 min and started to decrease afterwards. As the RCA process continued, the DNA hydrogel gradually grew and accumulated in the droplet. Therefore, the acoustic streaming velocity continuously decreased due to further increase of viscoelasticity. After 30 min from Lamb wave generation, the acoustic streaming velocity was measured as ~82% of the initial value, which indicates that viscoelasticity of the sample droplet increased (see Supporting Movie S1). After 60 min from Lamb wave generation, the acoustic streaming velocity decreased to ~48% of the initial velocity.

To validate the Lamb wave-based DNA amplification, RCA real-time fluorescence analysis was performed with the dengue negative and positive samples, as shown in Fig. 4(b). A stable fluorescence signal was reached in about 20 min. After that, positive control, which contains dengue pathogen oligonucleotides, showed gradually increased fluorescence intensity, whereas no fluorescence intensity increases were observed in the negative control without dengue pathogen oligonucleotides. In addition, to verify DNA hydrogel formation, RCA mixture with/without dengue pathogen oligonucleotides was incubated at 30 °C for 8 h, and DNA hydrogel formation during the RCA process was confirmed by pipetting (Fig. 4(b) Inset). In the Lamb wave-based device, nucleic acid amplification was detected qualitatively by decrease of the acoustic streaming velocities of particles induced by viscosity changes. To enable the quantitative evaluation, the velocity change should be compared to the quantitative increase of fluorescence intensity during PCR analysis depending on the concentration of target DNA for standardization. To evaluate the validity of the Lamb wave-based DNA amplification further, it will be worth comparing the RCA

product detection using the conventional methods such as agarose gel or polyacrylamide gel electrophoresis (PAGE).

To monitor the changes of the streaming velocities due to DNA hydrogel formation, the suspended particles in the sample droplet do not need to be fluorescence. Lamb wave-based device for molecular diagnosis can be utilized in POC settings or resource-limited environment without high-speed and fluorescent camera. Additionally, the time-dependent changes in the streaming velocities of the sample droplet can be visualized throughout the RCA process in real time.

In the Lamb wave device, the temperature increase in the sample is dependent not only on the applied voltage, but also on the distance from the electrode. Due to thermal resistance of the electrodes, temperature at the electrodes increases with applied voltages, which thermally affect the sample droplet. In the present device, the width of the electrode (w_{elec}) and the distance between the electrode and the sample droplet (d) were 6 mm and 5 mm, respectively, as shown in Fig. 2(b). The size and the arrangement of the electrodes can be further optimized for the use of our device at 30 °C with lower power consumption. Meanwhile, if low applied voltage can be used to achieve 30 °C, relatively low acoustic streaming velocity will be induced in the sample droplet. Then, it is expected that small difference in viscosity can affect the acoustic streaming velocity, thereby improving the device sensitivity. In addition, by modulating the applied voltage and the electrode design, different temperature ranges can be used, for example, 60–65 °C for LAMP, without considering the evaporation problem.

As the further optimization, the device parameters including the sample volume, the size and the concentration of suspending particles are required to be considered to enhance the sensitivity, the sequence specificity and the limit of detection as future work. With the high concentration of large-sized particles suspended in decreased sample volume, the device sensitivity is expected to be enhanced. Also, before applying the device to clinical samples, effects of unrelated DNA on the sample viscosity during RCA process and other acoustic interferences are required to be studied. With further optimization, the Lamb wave-based device can be applied to diagnose real virus sample, not the designed target pathogen DNA. Also, by using large area of electrodes, acoustic streaming can be induced simultaneously in multiple droplets, which is the most notable feature of the Lamb wave-based device compared to SAW device. Therefore, multiplexed detection of infectious diseases can be performed using various samples and templates for different disease targets including dengue, MERS, Ebola, Zika virus. Meanwhile, to enable the use of Lamb wave-based device for molecular diagnosis in point-of-care (POC) settings or resource-limited environment, large external instruments such as a signal generator, a power supply, and an amplifier can be manufactured as miniaturized, battery-powered module with the fixed working conditions of the frequency and the applied voltage (Rajapaksa et al., 2014).

In our experimental setup, as the contact angle increases, the acoustic streaming velocity has a tendency to increase. If the internal acoustic streaming can be induced in the droplet with high contact angle even with low applied voltage, the applicability of our device can be extended further to sample with high viscosity, for example, whole blood analysis and quality control of viscous oil.

4. Conclusion

In this study, we have described a novel Lamb-wave based device for detecting DNA amplification. The Lamb wave-based device was characterized using various parameters including the contact angle and the viscosity of the sample droplet. Due to Lamb wave-based temperature increase, the temperature reached to 30 °C at the applied voltage of 17 V, which is the optimal temperature for RCA process. The viscosity of the droplet affects the streaming velocity linearly, i.e., velocity decrease with increasing viscosity. Therefore, DNA hydrogel formation in RCA process could be monitored by the acoustic streaming velocity decrease due to viscosity increase. Using positive control samples containing target DNA, the acoustic streaming velocity showed notable decrease after 30 min and continuously decreased during the RCA process, while the acoustic streaming velocity remained uniform in negative control sample. In our simple and easily-fabricated Lamb wave-based device, RCA products can be effectively detected by using small volume of samples (10 μL) in short time duration (~30 min). Further studies are currently in progress for multiplexed detection of a variety of infectious disease including malaria, dengue, MERS, Ebola, and Zika.

Declaration of interests

The authors declare that they have no known competing financial interests or personal relationships that could have appeared to influence the work reported in this paper.

CRediT authorship contribution statement

Jeonghun Nam: Conceptualization, Data curation, Formal analysis, Writing - original draft. **Woong Sik Jang:** Formal analysis, Writing - original draft. **Jisu Kim:** Methodology, Formal analysis. **Hyukjin Lee:** Investigation, Resources, Writing - review & editing. **Chae Seung Lim:** Funding acquisition, Project administration, Resources, Supervision.

Acknowledgement

This study was supported by a government-wide R&D fund project for infectious disease research (HG18C0012).

Appendix A. Supplementary data

Supplementary data to this article can be found online at https://doi.org/10.1016/j.bios.2019.111496.

References

Allegranzi, B., Nejad, S.B., Combescure, C., Graafmans, W., Attar, H., Donaldson, L., Pittet, D., 2011. The Lancet 377, 228–241.
Brown, D., 2012. Open Source Physics comPADRE, USA.
Destgeer, G., Ha, B., Park, J., Sung, H.J., 2016. Anal. Chem. 88, 3976–3981.
Destgeer, G., Jung, J.H., Pakr, J., Ahmed, H., Sung, H.J., 2017. Anal. Chem. 89 (1), 736–744.
Guerrant, R.L., Walker, D.H., Weller, P.F., 2011. In: In: Dark, P.M., Dean, P., Warhurst, G. (Eds.), Tropical Infectious Diseases: Principles, Pathogens and Practice (Expert Consult—Online and Print), 3e. Vol. Saunders, vol. 13. Critical care, pp. 217 2009.
Guttenberg, Z., Müller, H., Habermüller, H., Geisbauer, A., Pipper, J., Felbel, J., Kielpinski, M., Scriba, J., Wixforth, A., 2005. Lab Chip 5, 308–317.
Jung, I.Y., You, J.B., Choi, B.R., Kim, J.S., Lee, H.K., Jang, B., Jeong, H.S., Lee, K., Im, S.G., Lee, H., 2016. Adv. Healthc. Mater. 5, 2168–2173.
Lee, H.Y., Jeong, H., Jung, I.Y., Jang, B., Seo, Y.C., Lee, H., Lee, H., 2015. Adv. Mater. 27, 3513–3517.
Loman, N.J., Constantinidou, C., Chan, J.Z., Halachev, M., Sergeant, M., Penn, C.W., Robinson, E.R., Pallen, M.J., 2012. Nat. Rev. Microbiol. 10, 599.
Luong, T.D., Nguyen, N.T., 2010. Micro Nanosyst. 2, 217–225.
Na, W., Nam, D., Lee, H., Shin, S., 2018. Biosens. Bioelectron. 108, 9–13.
Nam, J., Choi, H., Kim, J.Y., Jang, W., Lim, C.S., 2018. Sensor. Actuator. B Chem. 263, 190–195.
Rajapaksa, A., Qi, A., Yeo, L.Y., Coppel, R., Friend, J.R., 2014. Lab Chip 14, 1858–1865.
Reboud, J., Bourquin, Y., Wilson, R., Pall, G.S., Jiwaji, M., Pitt, A.R., Graham, A., Waters, A.P., Cooper, J.M., 2012. Proc. Natl. Acad. Sci. Unit. States Am. 109, 15162–15167.
Rezk, A.R., Friend, J.R., Yeo, L.Y., 2014. Lab Chip 14, 1802–1805.
Romanov, V., Davidoff, S.N., Miles, A.R., Grainger, D.W., Gale, B.K., Brooks, B.D., 2014. Analyst 139, 1303–1326.
Xu, G., Gunson, R.N., Cooper, J.M., Reboud, J., 2015. Chem. Commun. 51, 2589–2592.
Yeo, L., Rezk, A., 2017. Inf. MIDEM 46, 176–182.
Yonemoto, Y., Kunugi, T., 2014. Sci. World J. 2014, 647694.
Zilio, C., Sola, L., Damin, F., Faggioni, L., Chiari, M., 2014. Biomed. Microdevices 16, 107–114.